



Applicability conditions and experimental analysis of the variable stripe length method for gain measurements

L. Dal Negro ^{a,1}, P. Bettotti ^a, M. Cazzanelli ^{a,*}, D. Pacifici ^b, L. Pavesi ^a

^a *INFN and Dipartimento di Fisica, Università di Trento, Via Sommarive 14, I-38050 Povo, Italy*

^b *INFN and Dipartimento di Fisica e Astronomia, Università di Catania, Via Santa Sofia 64, I-95123 Catania, Italy*

Received 23 June 2003; received in revised form 29 September 2003; accepted 26 October 2003

Abstract

We discuss here some crucial issues related to the validity of the variable stripe length (VSL) method to measure optical gain in semiconductor materials and we especially point out the main experimental as well as conceptual difficulties arising when the VSL method is barely applied to low gain materials such as silicon nanocrystals (Si-nc) devised in a planar waveguide geometry. The variable stripe length method is revised carefully considering all the basic assumptions of its underlying one dimensional optical amplifier model, such as the gain saturation problem, the pump diffraction effects, and the inhomogeneous collection coupling of the amplified spontaneous emission. We will show how the standard one dimensional optical amplifier model has to be generalized in order to avoid undue artefacts as well as fundamental flaws. We indicate that, once the model has been properly modified, a more refined experimental analysis can be performed on the VSL experimental data yielding unambiguous gain values even in the case of planar waveguides made of low gain materials.

© 2003 Elsevier B.V. All rights reserved.

PACS: 78.67.Bf; 78.45.+h

Keywords: Nanocrystals and nanoparticles; Optical gain

1. Introduction

Optical gain coefficients can be measured by the variable stripe length (VSL) technique firstly introduced during the seventies [1]. The big advan-

tage of such a widely used experimental method is that no special sample preparation is needed and transparent as well opaque samples are equally suited for gain measurements. In addition, the basic principle of the technique is extremely simple: the one-dimensional amplifier model. However, the applicability range of this technique has not been deeply investigated so far. Special care is needed when measuring low gain materials and planar waveguide structures. Diffraction as well as stray light coupling effects can lead to artificial

* Corresponding author. Fax: +39-0461-881-696.

E-mail addresses: dalnegro@mit.edu (L. Dal Negro), kazza@science.unitn.it (M. Cazzanelli).

¹ Present address: Materials Processing Centre, Massachusetts Institute of Technology.

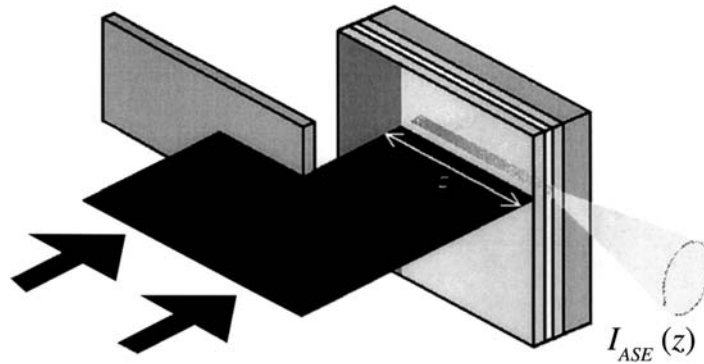


Fig. 1. Sketch of the variable stripe length configuration. The amplified spontaneous luminescence Intensity $I_{ASE}(z)$ is collected from the edge of the sample as a function of the excitation length z . The laser beam is focused on a thin stripe by a cylindrical lens.

gain values making the VSL technique highly misleading. To address all these potential sources of experimental as well as conceptual flaws, we propose here both a careful experimental strategy and a generalized approach based on a more complex modelling of the one dimensional optical amplifier scheme, relaxing all the simplifying hypothesis that originate the standard VSL model.

The aim of this work is intended to be twofold: on one side we want to carefully review the main assumptions that lay behind the apparently simple-looking VSL technique and, on the other side, we want to demonstrate that once the VSL data are carefully considered within a generalised one dimensional amplifier model, accurate and reproducible optical gain values can be deduced from planar active waveguides even in the low gain limit. The model system used in this work is a planar waveguide where the active core layer is formed by silicon nanocrystals (Si-nc) dispersed in SiO_2 [3–5]. We begin our analysis by reviewing the VSL technique method as applied to an amplifier rod. In the following sections we will modify this simple model in order to study optical gain in planar waveguide structures.

In the VSL method the sample is optically excited by an intense laser beam, which is focused by a cylindrical lens to form a narrow stripe on the sample surface. The length z of the stripe can be varied through a movable (variable) slit. An amplified spontaneous emission (ASE) signal I_{ASE} is collected from the edge of the sample as a function

of z (Fig. 1). As a result of population inversion achieved at high pumping rates, spontaneously emitted light is amplified and an intense, and partially coherent ASE signal grows up exponentially increasing the excitation length z . Distinctive characteristics of the ASE signal are that the ASE bandwidth is appreciably narrower than that of spontaneous emission and that the intensity growth exhibits a soft threshold behaviour versus power [2,3]. In addition, the presence of the ASE signal significantly shortens the luminescence decay time since the stimulated emission lifetime is inversely related to the flux of stimulating photons [3–5].

The ASE intensity increase versus z is usually described in a first approximation by a one dimensional optical amplifier model [6,7]. The one dimensional rod amplifier is a good approximation for VSL measurements applied to planar active waveguides when the gain coefficient is high. In fact the optical pumping geometry realizes a geometry very similar to the one found in gain-guided stripe semiconductor lasers which are widely used in photonics. Here, the lateral mode confinement is realized by confining the inverted region, i.e. the gaining region, to a narrow stripe by spatial confinement of the injected current. The limits of the rod amplifier model are evident when the gain coefficient is low (few cm^{-1}) as discussed in Section 5.

Considering a one dimensional amplifier rod of cross sectional area S and length L , a propagation

intensity equation can be written for the spontaneous emission [6,7]:

$$\frac{dI}{dz} = (\Gamma g_m - \alpha)I + (A_{sp}N^* \times hv)[\Omega(z)/4\pi], \quad (1)$$

where g_m is the gain of the material, Γ is the confinement factor of the waveguide structure, α is the propagation loss coefficient, A_{sp} is the spontaneous emission rate, N^* is the excited state population density and hv is the energy of the emitted photon. $\Omega(z)$ is the solid angle subtended by the exit amplifier face as seen from the differential element dz in the amplifier (see Fig. 2). The factor $\Omega(z)/4\pi$ on the right hand side of Eq. (1) is the fraction of spontaneous emission from element dz that propagates along the amplification axis. Eq. (1) can be analytically integrated to obtain the ASE intensity at the exit face of the amplifier *only under specific working hypothesis*.

Since most of the significant ASE emission arises from the emitting elements near $z = L$, which experience the largest single pass gain, it is always assumed that $\Omega(z) \cong \Omega = S/L^2$ (see Fig. 2). More generally, the z -dependence of $\Omega(z)$ strongly affects the collection efficiency of the ASE signal. The condition $\Omega(z) \cong \Omega$ corresponds to the assumption of a constant collection efficiency, hypothesis which is satisfied for optical amplifiers based on optical fibres or two-dimensional waveguides, but which is not fulfilled in the case of planar waveguides where the modes spread in the waveguide plane introducing a z dependence in the otherwise constant collection efficiency (described by the variable $\Omega(z)$)

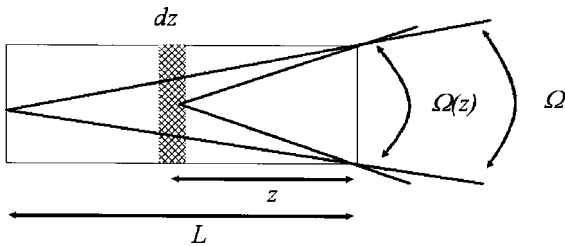


Fig. 2. Top view of the excited stripe on the surface of the planar waveguide. L is the total length of the amplifier, z is the slit edge position projected on the sample surface, dz is the integration element, $\Omega(z)$ is the solid angle defined by the exit facet of the amplifier and the point z of the slit edge on the sample surface. $\Omega(z) = \Omega$ when $z = L$.

factor). In addition, inhomogeneous coupling can also arise as a result of an inappropriate choice of the numerical aperture (and depth of focus) of the collection optics used in the experiments, or as a result of the collection of surface (non-guided) light emission as will be discussed in later sections.

The first assumption of the simple one dimensional amplifier model consists therefore in the homogeneous collection efficiency of the edge emitted radiation, *assuming a light collection efficiency that does not depend on the pumping length z* .

In addition to this requirement, to find an analytical solution of Eq. (1) a constant gain coefficient along the amplifier axis is usually assumed. However, under certain circumstances, a spatial dependence in the gain coefficient is observed. Examples are related to the gain saturation problem or when a non-homogeneous pump intensity profile is used. We will discuss these effects in the next sections. This second general hypothesis can be referred to as the *homogeneity of the gain and pump intensity over the whole pumping length z* . Only under these strict assumptions, Eq. (1) can be integrated with the boundary condition $I_{ASE}(0) = 0$. In the case of an amplifier formed by an active waveguide, the solution to Eq. (1) is

$$I_{ASE}(z) = \frac{J_{sp}(\Omega)}{g_{mod}} (e^{g_{mod}z} - 1), \quad (2)$$

where $J_{sp}(\Omega) = \left(\frac{A_{sp}hv\Omega N^*}{4\pi}\right)$ is the spontaneous emission intensity emitted within the solid angle Ω and g_{mod} is the *net modal gain* of the material, defined as $g_{mod} = \Gamma g_m - \alpha$. For simplicity of notation, we put $g_{mod} = g$ hereafter. From a fit of the experimental data with Eq. (2), the modal gain g can be deduced for every wavelength within the spontaneous emission spectrum [8].

2. Gain saturation

In the derivation of Eq. (2) we have assumed that g is independent of z . This is not true in general, because the ASE intensity itself could significantly deplete the excited state population N^* reducing the gain as the signal intensity builds up along the amplification axis. This is known as the gain saturation effect [6].

In order to take into account the effect of gain saturation, the ASE propagation equation (1) can be modified by replacing the small signal gain g_0 (independent on the signal intensity) and the small signal excited state population N_0^* with the corresponding relations for the intensity dependent optical gain $g(z)$ and population density $N(z)$. In the case of homogeneous amplifier systems the corresponding expressions are [6]:

$$g(z) = \frac{g_0}{1 + \frac{I(z)}{I_{\text{sat}}}} \quad \text{and} \quad N(z) = \frac{N_0^*}{1 + \frac{I(z)}{I_{\text{sat}}}},$$

respectively, and Eq. (1) can be rewritten as

$$\frac{dI}{dz} = \frac{g_0 I}{1 + \frac{I(z)}{I_{\text{sat}}}} + \left(A_{\text{sp}} \frac{N_0^*}{1 + \frac{I(z)}{I_{\text{sat}}}} \times h\nu \right) \times [\Omega/4\pi], \quad (3)$$

where for simplicity we have set $\alpha = 0$, $\Gamma = 1$ and Ω constant.

In the case of inhomogeneous amplifier systems, which could correspond to our test model where Si-nc have a wide size distribution, the intensity-dependent gain coefficient can be obtained by integrating the contributions from the different frequency components (each of which saturates differently depending on the detuning from the central gain frequency) and the saturation formula [6] $g(z) = \frac{g_0}{\sqrt{1 + (I(z)/I_{\text{sat}})}}$ is usually assumed. The corresponding ASE propagation equation is thus modified to:

$$\frac{dI}{dz} = \frac{g_0 I}{\sqrt{1 + \frac{I(z)}{I_{\text{sat}}}}} + \left(A_{\text{sp}} \frac{N_0^*}{\sqrt{1 + \frac{I(z)}{I_{\text{sat}}}}} \times h\nu \right) [\Omega/4\pi]. \quad (4)$$

We notice here that the gain saturation expressions used in Eqs. (3) and (4), even if derived within the hypothesis of simple three and four levels models, are often applicable far outside the range of validity of these simplified models [6], and Eqs. (3) and (4) can be assumed to hold without loss of generality.

Our model system is based on Si-nc and most of the reported experimental evidences of optical gain in Si-nc systems have been related to the presence of an effective four levels system due to strong structural relaxation of small oxygen-saturated Si-nc involving localized states [4,5,8,9]. Thus we consider

the signal saturation intensity of a four level amplifier $I_{\text{sat}} = \hbar\omega/\sigma\tau$, where σ is the emission cross section of the Si-nc and τ is the Si-nc radiative lifetime.

The results of the numerical integration of Eqs. (3) and (4) are shown in Figs. 3(a) and (b) where we plot the ASE intensity and the gain coefficient versus the pumping length of the VSL experiment for both the gain saturation models. The gain coefficient remains equal to the small signal gain g_0 (here we have considered $g_0 = 50 \text{ cm}^{-1}$) until a critical pumping length, saturation length z_{sat} , is

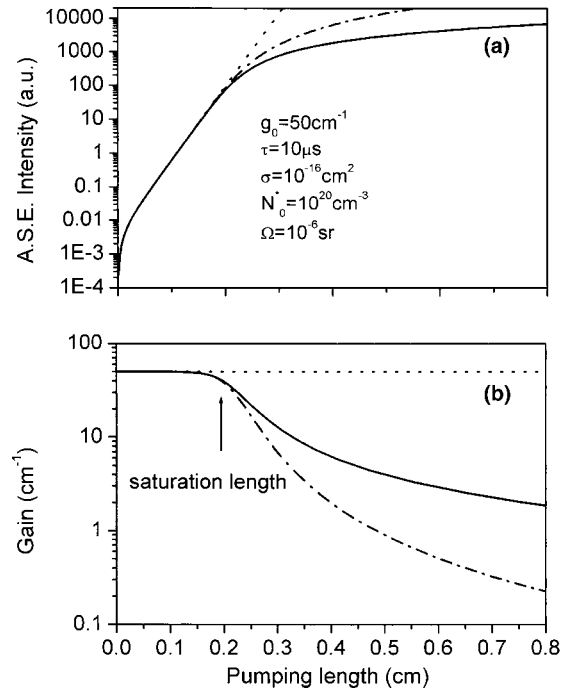


Fig. 3. Panel (a): Amplified spontaneous emission (ASE) intensity versus the length of the photo-excited region which results from solving Eq. (3) considering a small signal gain coefficient $g_0 = 50 \text{ cm}^{-1}$ and homogeneous gain saturation (solid line), solution of Eq. (4) for the case of inhomogeneous gain saturation model (dash-dot line), solution of the simple one dimensional amplifier model without the contribution of gain saturation (dotted line). Panel (b): Spatial dependence of the optical gain coefficient in the case of inhomogeneous saturation (dash-dot line), homogeneous gain saturation (solid line) and without the gain saturation effect (dotted line). A saturation length $z_{\text{sat}} = 0.2 \text{ cm}$ can be deduced for the simulation parameters used: signal wavelength $\lambda = 750 \text{ nm}$, $\Omega = 10^{-6} \text{ sr}$, Si-nc density $N_0^* = 10^{20} \text{ cm}^{-3}$, Si-nc emission cross section $\sigma = 10^{-16} \text{ cm}^2$, Si-nc lifetime $\tau = 10 \mu\text{s}$.

achieved (in the example considered $z_{\text{sat}} = 0.2$ cm). For $z > z_{\text{sat}}$, g decreases and, eventually, vanishes. In this situation, the ASE intensity starts to deviate from the usual exponential increase according to a characteristic saturation behaviour. It is interesting to note here that the onset of gain saturation (the critical length) is almost independent on the saturation model considered. In fact, only the decrease of the intensity dependent gain beyond the saturation length reflects the choice of the actual saturation model. In the example of Fig. 3, a saturation length of 0.2 cm can be deduced, regardless of the details of the saturation mechanism (homogeneous or inhomogeneous).

Our model can be used to estimate the maximum gain-length product gz_{sat} in order to avoid the onset of gain saturation in the VSL experiments. From Fig. 3, $gz_{\text{sat}} = 10$ can be deduced. This result is consistent with the quantitative estimation of the critical gz_{sat} product derived in [6] under the assumption of a four level system:

$$gz_{\text{sat}} = \log \left(\frac{\lambda^5 I_{\text{sat}}}{\pi h c^2 \Omega \Delta \lambda} \right), \quad (5)$$

where λ is the emission wavelength and $\Delta \lambda$ is the emission linewidth.

It is clear from Eq. (5) that large-core amplifiers, subtending large solid angles, are most susceptible to the saturation of ASE signal, since a larger flux of spontaneously emitted photons can be sustained. The application of Eq. (5) to the case of Si-nc emitting at 750 nm with a typical luminescence width of 130 nm (and a typical $\Omega = 10^{-6}$) yields $gz_{\text{sat}} \approx 10$, in agreement with the gain-length product estimated on the basis of our simple saturation model.

In addition, Eq. (5) can be significantly simplified in the case of high gain materials (gain-length products $gz_{\text{sat}} > 1$). Defining a luminescence quantum yield $\eta = \tau A_{\text{sp}}$, and imposing the gain-saturation condition $I_{\text{ASE}} = I_{\text{sat}}$ we can obtain:

$$gz_{\text{sat}} \approx \log \left(\frac{4\pi}{\eta \Omega} \right). \quad (6)$$

Eq. (6) shows that materials with high quantum yields have small gain-length product, strongly reducing the applicability range of the VSL technique.

We point out that similar gain-length product estimations can be deduced by applying the Lindford formula, that is a general relation containing the integral information over the whole spectral emission band. In the case of inhomogeneously broadened lasers one has [2]:

$$I_{\text{ASE}} = \eta I_s \left(\frac{\Omega}{4\pi} \right) \frac{(G-1)^{\frac{3}{2}}}{(G \ln G)^{\frac{1}{2}}}, \quad (7)$$

where G is the single pass gain $G = \exp(gz)$ and I_{ASE} is the integrated emission intensity. For example, for Si-nc where gain coefficients ranging from 10 to 100 cm^{-1} have been measured by VSL [3–5,8,9], a maximum pumping length of the order of 0.1 cm (when $g = 100 \text{ cm}^{-1}$) can be calculated, in good agreement with the estimate deduced from the integration of Eqs. (3) and (4).

3. Pump diffraction effects

A second important requirement for the validity of Eq. (2) is that of a constant pumping excitation intensity. Here we discuss an example which arises due to Fresnel diffraction effects caused by the edge of the slit [10]. Clearly these diffraction effects can be avoided by placing the slit very near to the sample surface [5]. However not always this is possible due to experimental constraints. We suggested a simple way to characterise and control experimentally diffraction effects [3,4]. It is based on the measure of the diffused pump light intensity as a function of the slit position. This measurement is extremely easy to perform within a standard VSL set-up, since it can be performed exactly as a VSL measurement (in the 90° configuration) by collecting the diffused pump laser light as a function of z .

We tested this approach by using a Si-nc waveguide produced by PE-CVD deposition followed by a high temperature annealing treatment (Fig. 4) [11]. Fig. 5 shows the results of a VSL measurement where the signal has been collected both at the pump wavelength (365 nm, hollow triangles) and at the ASE wavelength (750 nm, solid circles). The full line in Fig. 5 is a calculation of the diffracted pump beam within a Fresnel approximation. A good agreement between data and

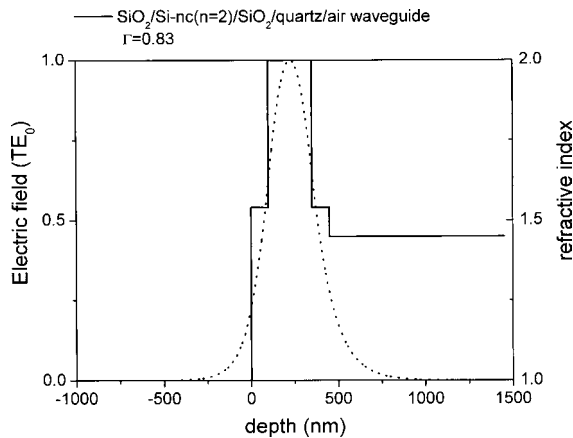


Fig. 4. Spatial mode profile of the waveguide structure for one representative silicon nanocrystals (Si-nc) sample. Calculation has been performed by assuming a refractive index of 2 for the Si-nc rich region and an effective 4 layers planar waveguide.

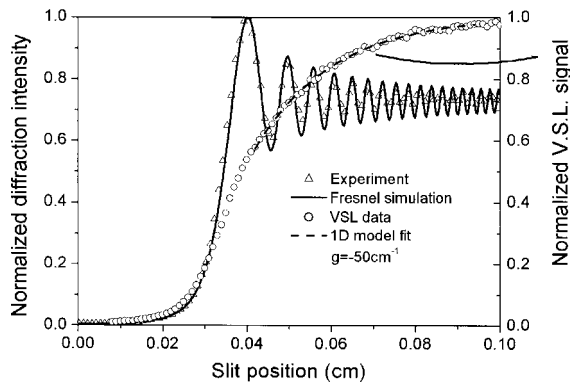


Fig. 5. Amplified spontaneous emission (ASE) at 800 nm (solid circles) and scattered pump laser signal at 365 nm (open triangles) simultaneously measured as a function of the excitation length. The VSL signal has been normalized over its saturation value. The solid line is the result of a simulation of the Fresnel diffraction curve using the experimental parameters (normalized to one). Pump laser beam waist on the cylindrical lens was 1.5 mm. As half of it was intercepted by the slit, a rectangular excited region on the sample surface of $10 \mu\text{m} \times 0.8 \text{ mm}$ was used. The laser wavelength was 365 nm and the pump intensity on the sample surface was 50 W/cm^2 . The variable slit was placed at a distance of 3 cm from the sample surface. The sample was a $\text{SiO}_2/\text{SiO}_2:\text{Si-nc}/\text{SiO}_2$ waveguide deposited on top of a quartz substrate. Experimental details are given in [4]. The line on the open circles is a fit to the data with Eq. (2). The gain parameter deduced from the fit is reported in the figure.

calculation can be observed. In Fig. 5, the pumping intensity can be considered constant on the sample only for $z > 0.04 \text{ cm}$. Note that we arbitrarily set the origin of the z -axis in a region where no signal was measured. In the region where diffraction effects are dominant ($z < 0.04 \text{ cm}$) I_{ASE} increases exponentially with z . A fit of the data with Eq. (2) in this z -region will yield an artificial positive gain coefficient of about 100 cm^{-1} . This is an artefact which has a very peculiar signature: the artificial gain value is almost independent on the pump intensity on a wide pump intensity range. Gain has to depend on the pump intensity since population inversion strongly depends on the pumping conditions. On the contrary, if the data in Fig. 5 are fitted for $z > 0.04 \text{ cm}$, negative gain values (i.e. optical losses) of -50 cm^{-1} are deduced from the fit with Eq. (2) (solid curve). Our proposed *pump diffraction analysis* is of great help in understanding the initial position from which the VSL data can be fitted within the approximations of the one dimensional model of Eq. (2).

The ending points in this fit are chosen on the basis of the saturation length (as discussed before) and of the laser waist size, since an artificial saturation effect can arise also from its Gaussian intensity profile. In our experiment we used an UV extended Ar laser with a Gaussian beam profile. To avoid the inherent inhomogeneity of the Gaussian profile, we used the conservative approach to place the sample edge in the middle of the transversal laser waist. Even if this strategy leads to an underestimation of the actual gain values, it allows to rule out serious experimental flaws such as apparent gain observations and saturation regime.

4. Coupling effects

A third important issue concerning VSL measurements is that of the constant coupling of the guided emission with the detection optics. The coupling efficiency must be independent on the pumping length z in order to apply Eq. (2), as already pointed out.

On the contrary, in the case of planar waveguides the coupling efficiency is not independent

on the excitation length z since the in-plane spreading of the emission originates inhomogeneous coupling effects with the detection optics that can strongly affect the experimental results. In addition, for excitation near to the sample edge (short z), the excited and amplified optical modes are less collimated (see Fig. 2) with respect to the modes excited at large distances (large z).

To experimentally check the homogeneity of such a coupling, a comparison of VSL results with that of the “shifting excitation spot” (SES) technique has been proposed [12]. The SES method was originally introduced in [13,14] to measure the optical losses in a laser waveguide structures. Briefly, the SES method consists in exciting the sample on a small spot area, whose lateral position can be shifted with respect to the sample edge, and detecting the intensity of the light emitted from the sample edge (Fig. 6). Since the emitted light travels along a region which is not photo-excited, the collected intensity as a function of the spot position z decreases according to a characteristic attenuation law. In the simple case of collimated optical beams (like in optical fibers) the intensity decay follows the exponential Lambert–Beer’s law. Since the optical mode remains collimated while

propagating, the collection efficiency is independent on the exciting spot position thus allowing for an easy measurement of the loss coefficient α . On the contrary, in the case of a planar waveguide, the optical mode has an angular spread in the waveguide plane which depends on the exciting spot position z (see Fig. 6(b)).

The collection efficiency of the emitted light for both VSL and SES experiments will thus be geometrically limited by the finite numerical aperture (NA) of the collection system in the waveguide plane, where $\text{NA} = \sin(\varphi)$ and the angle φ is defined in Fig. 6(b). The analysis is simple for the SES geometry, if we assume a cylindrically symmetric collection system (a simple spherical lens, a microscope objective, etc.) with a lateral dimension d (parallel to the waveguide plane) and positioned at a fixed distance x from the sample edge (see Fig. 6(b)). Light from the point z is isotropically emitted in the waveguide plane, i.e. over an angle 2π , and propagates along the waveguide plane. Let us define the collection efficiency $\rho(z)$ of the optical system by the ratio of the transversal acceptance angle of the collection system $\varphi(z)$ to the total angle: $\rho(z) = \varphi/2\pi$. Thus:

$$\rho(z) = \frac{\varphi}{2\pi} = (1/2\pi) \tan^{-1} \left(\frac{d/2}{x+z} \right). \quad (8)$$

Eq. (8) simplifies to $\rho(z) \propto 1/z$ when the exciting spot position is well inside the sample (or $z \gg x$).

Hence for planar waveguides the measured luminescence signal in a SES experiment will be proportional to $\rho(z) \exp(-\alpha \cdot z)$, which reduces to $\propto \exp(-\alpha \cdot z)/z$ for $z \gg x$ [15]. It is interesting to note that, in the more general case discussed here, the standard Lambert–Beer’s law can be extended to the case of inhomogeneous spatial coupling by writing:

$$\frac{dI}{dz} = -\alpha I [1 + \rho(z)], \quad (9)$$

where the effect of the mode divergence is fully taken into account through the coupling function $\rho(z)$.

To study the experimental coupling conditions in our samples, we have applied SES technique to a Si-nc planar waveguide with a core thickness $w_1 = 250$ nm and two silica cladding layers with

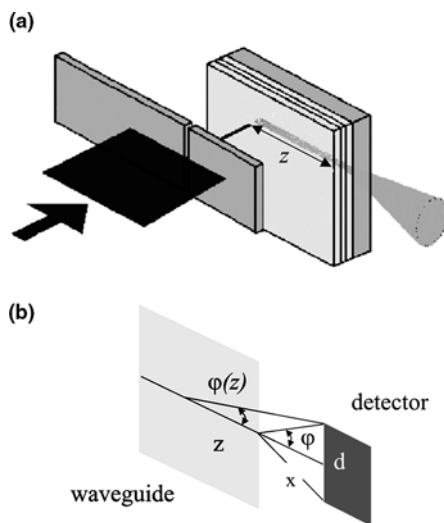


Fig. 6. (a) Sketch of the shifting excitation spot technique (SES). The spotted excitation is obtained by using $40 \mu\text{m}$ pin-hole. (b) Projection on the waveguide plane and definition of the relevant quantities to estimate the collection efficiency.

thickness $w_c = 100$ nm deposited on a quartz substrate (Fig. 4). We excited the luminescence by a tiny laser spot with an estimated diameter of ≈ 100 μm on the sample surface and with a wavelength of 365 nm (UV extended Argon laser). The laser spot was formed by passing the beam through a movable pin-hole just after the cylindrical lens used in the VSL and near to the sample surface. Collection of the luminescence exiting from the edge and guided by the sample was performed via a 40 \times microscope objective with NA = 0.65, the same aperture that we use for VSL measurements. The transversal numerical aperture of the waveguide was estimated to be $\text{NA} \approx \lambda/\pi w_1 = 0.44$, allowing total collection of the edge emitted light.

Fig. 7 shows SES and VSL measurements performed on the same sample. In SES measurement shown in Fig. 7(a) the luminescence signal decreases exponentially when sweeping the laser spot

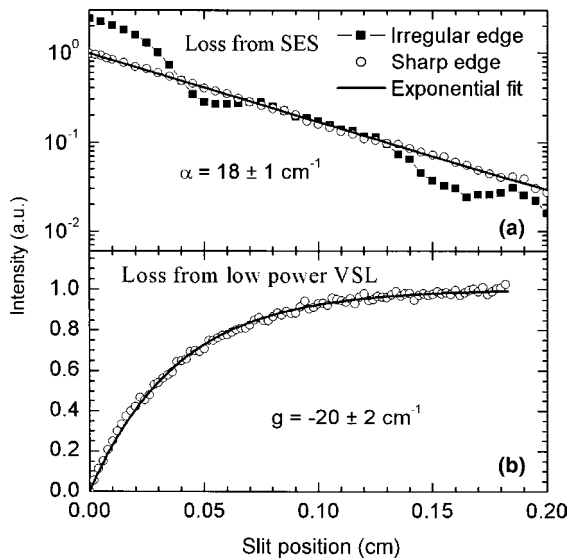


Fig. 7. Edge emission intensity at 750 nm versus slit position for SES measurements (Fig. 7(a)) and versus slit width for VSL measurements (Fig. 7(b)). The sample was a $\text{SiO}_2/\text{SiO}_2:\text{Si-nc}/\text{SiO}_2$ waveguide deposited on top of a quartz substrate [4]. SES measurements on an irregular edge (filled squares) and on a sharp edge (open circles) of the sample are shown for comparison. Fit of the experimental data with the modified Beer's law for SES data or with Eq. (2) for VSL data are reported on the graph.

from the sample edge (open circles). An effective loss parameter α can be extracted which is related to both absorption and propagation losses in the waveguide. Moreover, this α value coincides within the experimental errors with the optical loss value obtained from VSL measurements performed at the same wavelength (Fig. 7(b)), when using a low pump power in a spectral region with a negligible absorption due to the Si nanocrystals. This is an important consistency proof showing that under our experimental conditions the coupling efficiency both in VSL and SES measurements are identical over the pumping range. This crucial observations allow us to rule out from an experimental point of view any artificial effect due to uncontrolled coupling conditions during the VSL experiments. It is worth noticing that also the quality (roughness and imperfections) of the sample edge significantly affects the measured SES profiles: indeed complex oscillatory behaviour is observed for a damaged edge (solid squares in Fig. 7(a)) [4].

Interestingly, [12] reported that the SES signal can increase when sweeping the excitation spot away from the sample edge, yielding to artificial gain values when VSL sweeps are performed. We have also observed this effect experimentally, but only under the following conditions: (i) when the optical axis of the waveguide formed an angle different from zero with respect to the optical axis of the collecting lens (*geometrical misalignment*); (ii) when the focal plane of the objective was positioned well within the sample (Fig. 8).

The latter condition deserves a detailed discussion. When the objective focal plane is placed within the sample so that it can be entirely crossed by the Gaussian excitation spot during a SES sweep, then (accordingly to the depth of field of the objective used) an additional non-constant light coupling contribution can modify the experimental conditions giving rise to artefacts in the SES and VSL measurements. The light collection efficiency can increase easily with increasing the pump length (as in [12]) or even remain constant in a large range of pumping length depending on the excitation spot size (the transversal beam waist) and objective numerical aperture NA (or depth of field D , according to the approximate relation $D \approx \lambda/\text{NA}^2$).

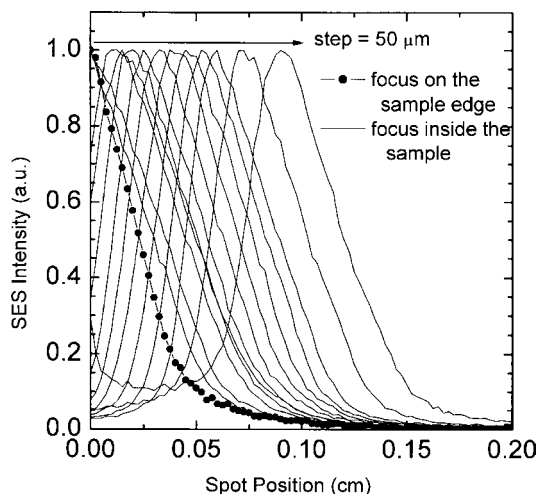


Fig. 8. Edge emission versus spot position for different positioning of the collecting objective focal plane. The focal plane was moved from the sample edge into the sample with a constant step of $50 \mu\text{m}$. SES emission was collected at a detection wavelength of 750 nm . Closed circles refer to SES measurement performed with the focal plane on the sample edge. Continuous lines are for SES measurements under wrong focusing conditions. The experimentally measured losses are $\alpha = -45 \pm 5 \text{ cm}^{-1}$ (dotted line).

This is experimentally demonstrated in Fig. 8, where SES measurements are performed for different locations of the objective focal plane. When the focal plane is correctly placed on the sample edge or far from it, an exponential decrease of the signal is measured (closed circles). However, when the focal plane is moved into the sample, the luminescence signal initially increases due to the increased overlap between the laser spot and the depth of field of the objective and then starts to decrease (continuous lines).

Another explanation of the anomalous increases observed in [12] can be looked for in the effect caused by the mode propagation in the waveguide. As the light is excited at longer z the propagating optical mode is more and more collimated in the waveguide and hence is detected more effectively by the collecting system. Waveguide mode filtering effects have been indeed reported [15]. Then when the mode is stable the effect of the propagation losses become dominant and a decrease in the intensity can be observed.

The interplay between all the different inhomogeneous coupling contributions considered so far can be indeed very complex. In the next chapter we will try to describe it from a simple phenomenological perspective to show that experimental artefacts (apparent gain) can easily arise when all these issues are not carefully considered.

However, when a careful comparative analysis between VSL and SES is performed, reliable gain values can be extracted also in the case of active planar waveguide samples. Fig. 9 shows the VSL results obtained on silicon nanocrystal waveguides [4]. All the previously discussed sources of experimental artefacts has been carefully ruled out in the results of Fig. 9. We observed losses at low pump power and optical gain at high pump power, keeping fixed all the other experimental conditions. We believe that this *loss/gain switch with increasing pump power* is a very robust test to be applied when VSL gain measurement has to be performed in low gain planar waveguides. In fact, all the possible artificial gain sources that we reviewed in the preceding sections necessarily yield unphysical power independent gain values.

5. Generalised one dimensional model

As we have seen in the preceding sections, the simple one dimensional optical amplifier model can fail when barely applied to small gain planar optical waveguides and special experimental cares have to be paid. To that purpose, we have suggested many experimental strategies in order to overcome these limitations and we have demonstrated their validity in the case of silicon nanocrystal waveguides.

Since we already discussed the physical origin of most of the possible experimental flaws, we will try to modify Eq. (1) in order to take into account all these effects from the beginning and motivate our experimental procedures within a more general propagation model. In addition, the experimental data in Fig. 9 will be reproduced within a modified SES model reinforcing our physical explanation of the inhomogeneous coupling effect.

The effect of Fresnel pump diffraction, the gain saturation, the different artefacts due to modal

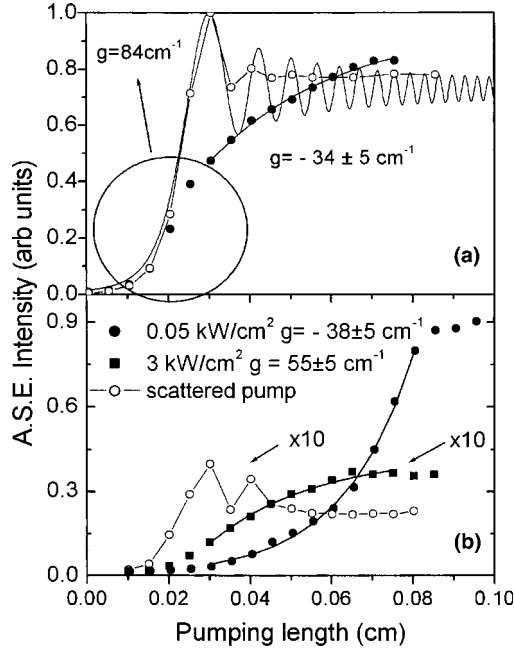


Fig. 9. Panel (a): Edge ASE emission at 800 nm (solid circles) and scattered pump laser signal (open circles) simultaneously measured as a function of the excitation length. The pump laser was focused on the sample surface through a cylindrical lens. The beam waist of the pump laser on the cylindrical lens was 0.9 mm, which resulted in a rectangular excited region on the sample surface of $10 \mu\text{m} \times 0.45 \text{ mm}$. The laser wavelength was 365 nm and the pump intensity on the sample surface was 50 W/cm^2 . A variable slit was placed at a distance of 7 cm from the sample surface. The sample was a $\text{SiO}_2/\text{SiO}_2:\text{Si-nc}/\text{SiO}_2$ waveguide deposited on top of a quartz substrate. For Fig. 9(a) the Si-nc were formed by annealing at 1250°C for 1 hr a SiO_x layer with 39% Si content. For Fig. 9(b) the Si-nc were formed by annealing at 1200°C for 1 hr a SiO_x layer with 39% Si content. Experimental details are given in [4]. Data were fitted with Eq. (2) in two different regions. The gain parameters deduced are reported in the figure. Panel (b): The ASE signal measured at 750 nm under 3 kW/cm^2 (solid squares) or 50 W/cm^2 (solid circles) pump intensity excitation. The line is a fit to the data with Eq. (2). Open circles refer to the scattered pump light used to define the origin of the fit.

divergence and inhomogeneous collection coupling efficiency can be included in a generalized one dimensional model through additional spatial dependent coefficients. We can write a generalized propagation equation as follows:

$$\frac{dI}{dz} = [g(z)\xi(z) - \alpha]I + [\xi(z)A_{\text{sp}}N(z)^*h\nu] \times [\beta_1(z) + \beta_2(z)], \quad (10)$$

where $\xi(z)$ is the normalized Fresnel diffraction intensity profile, $g(z)$ is the spatial dependent gain coefficient, $N(z)^*$ is the spatial dependent excited state population density (with the same saturation behaviour as $g(z)$), $\beta_1(z)$ represents a spatial dependent collection factor arising from the planar waveguide mode spreading (the guided optical modes are not collimated beams in the plane of the waveguide as discussed before) and $\beta_2(z)$ is the Gaussian coupling efficiency originating from the spatial laser intensity profile. Since the coupling efficiency function $\rho(z)$ introduced in the previous section can be approximated by a straight line we have assumed for simplicity a β_1 coupling efficiency that increases (decreases) according to $\beta_1 = \frac{\Omega}{4\pi} \pm B \times z$ where the B factor is $B = (M - 1) \times \frac{\Omega}{4\pi L_{\text{end}}}$,

M is the fraction of inhomogeneous coupling ($M = 1, 2, \dots, n$) and L_{end} is the maximum slit length in the VSL experiment. The \pm , in the collection term describes the increase or the decrease in the actual collection efficiency originating from better mode guidance (spatial mode collimation) and in-plane mode spreading respectively. The β_1 spatial dependent function used in this simple approximation implies that the collection efficiency increases (decreases) linearly as a result of mode guiding (spreading) in the waveguide plane until a certain fraction M of the initial constant emission solid angle Ω is reached at the maximum slit length L_{end} . The condition $M = 1$ implies constant coupling for all z . The term $\beta_2(z)$ is given by a Gaussian function that reproduces the laser spot. By numerical integration of Eq. (10), it is possible to reproduce all the spurious effects that we characterised experimentally. Fig. 11 shows some results considering the case of linear increase in the light coupling. We used a waveguide with 20 cm^{-1} of optical losses (I_{ASE} vs z from Eq. (2) shown in Fig. 10 as dashed curve) to emphasize that all the additional effects included in Eq. (10) can lead to artificial gain values even in the case of a passive waveguide structure (with no gain). When the effects of Fresnel diffraction are introduced in Eq. (10) through $\xi(z)$, an exponential rising edge appears in I_{ASE} (Fig. 11(a), solid line). This effect becomes even more steep when the Gaussian coupling factor β_2 is introduced in the model (Fig.11(a),

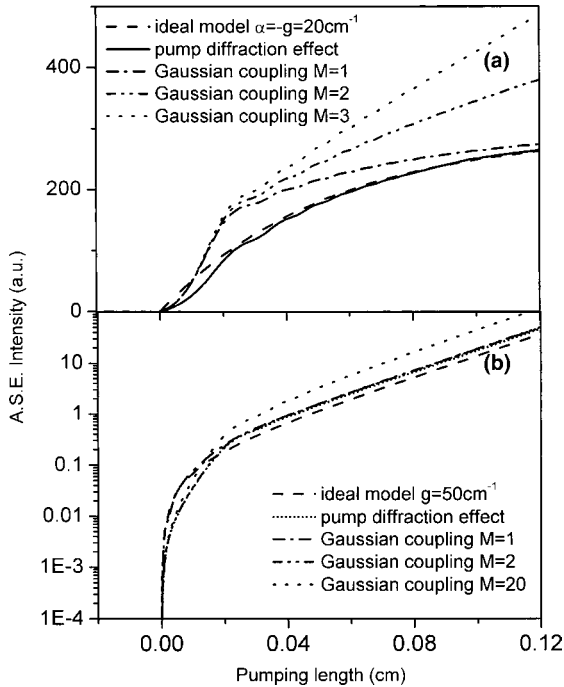


Fig. 10. Panel (a): Simulation of the VSL signal assuming 20 cm^{-1} of optical losses (dashed line). Simulation of the VSL signal considering the generalised model of Eq. (10) with the effect of the pump Fresnel diffraction only (solid line) and considering additionally the effect of inhomogeneous coupling due to the wrong focal position of the collecting objective (dash-dot line). Simulation of the VSL signal assuming Fresnel diffraction effects, inhomogeneous Gaussian coupling and additionally the mode spreading in the waveguide plane up to $M = 2$ (dash-dot-dot line). Simulation of the VSL signal assuming Fresnel diffraction effects, inhomogeneous Gaussian coupling and additionally the mode spreading in the waveguide plane up to $M = 3$ (dotted line). Panel (b): Simulation of the VSL signal assuming $g = 50 \text{ cm}^{-1}$ of optical gain (dash-dash-dot line). Simulation of the VSL signal considering the generalised model of Eq. (10) with the effect of the pump Fresnel diffraction only (short-dot line) and considering additionally the effect of inhomogeneous coupling due to the wrong focal position of the collecting objective (dash-dot line). Simulation of the VSL signal assuming Fresnel diffraction effects, inhomogeneous Gaussian coupling and additionally the mode spreading in the waveguide plane up to $M = 2$ (dash-dot-dot line). Simulation of the VSL signal assuming Fresnel diffraction effects, inhomogeneous Gaussian coupling and additionally the mode spreading in the waveguide plane up to $M = 20$ (dotted line).

dash-dot line) and can lead to artificial gain values. When $M = 2$ is used in Eq. (10) the VSL curve is strongly modified even outside the diffraction range

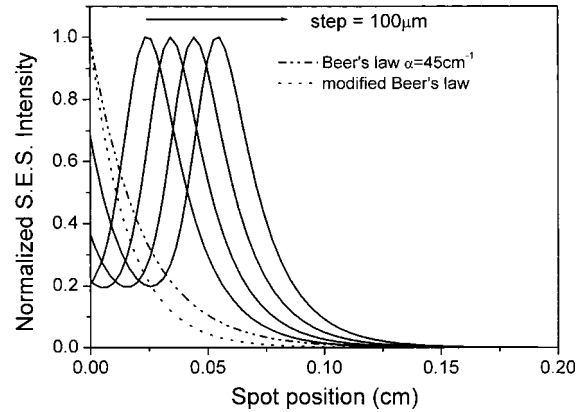


Fig. 11. Simulation of the SES signal considering the model of Eq. (11) for different spatial positions of the Gaussian laser beam waist with respect to the sample edge. The waist has been considered $100 \mu\text{m}$ wide. Losses of 45 cm^{-1} have been considered. SES signal as obtained from the Beer's law (dash-dot-dot line), SES signal as obtained from the solution of the modified Beer's law (dotted line). With reference to the schematics in Fig. 6(b) we have considered the experimental parameters $d = 0.3 \text{ cm}$ and $x = 0.1 \text{ cm}$.

(Fig. 11(a), dotted line). When $M = 2$ an artificial gain curve can arise because of the non-constant coupling (Fig. 11(a), dash-dot-dot line). For $M = 3$ (dotted line) the effect becomes dramatic. All these apparent gain curves only reflect the inhomogeneous light coupling of the edge emitted signal [12].

The coupling effects are therefore crucial for the estimation of low gain and loss values from the VSL analysis. However, when the gain values are high enough, all these spurious effects turned out to play a minor role and the VSL curves obtained within the simple one dimensional optical amplifier and the generalised model given by Eq. (10) are in good agreement under a wide range of perturbation parameters. A non-constant coupling with a M as high as 20 gives rise to only minor changes in the ideal VSL curves (see Fig. 11(b), dotted line). Our numerical simulations suggest that the VSL curve can be described accurately within the one dimensional optical amplifier model if the gain values are bigger than $20\text{--}30 \text{ cm}^{-1}$.

Dramatic modifications of the standard loss behaviour can also be deduced in the case of the SES technique when we extend the modified Lambert–Beer's law of Eq. (9) to a more general

form that takes into account the inhomogeneous Gaussian coupling contribution. This term arises from the effect of the finite depth of field D of the collecting system when its focal plane is shifted relatively to the excitation spot position, and we can write:

$$\frac{dI}{dz} = -\alpha[I + \rho(z)I] \times \left(\frac{\rho(0) - \beta_2}{\rho(0)} \right), \quad (11)$$

where the interplay between the two coupling mechanisms described by $\beta_1(0) \propto \rho(0)$ and β_2 is such that Eq. (11) can switch from an attenuation behaviour (when $\beta_1 > \beta_2$) to an exponential growth (when $\beta_1 < \beta_2$). Since the excitation spot is described by a Gaussian function with vanishing tails the regime described by Eq. (11) will eventually switch again into attenuation, exactly describing the experimental situation (see Fig. 11).

By solving Eq. (11), it is possible to reproduce the experimental data of Fig. 8 accurately. The simulation results are shown in Fig. 11. Analogously to the experimental situation described in Fig. 8, we performed a 100 μm sweep (starting from the sample edge, dash-dot line in Fig. 11) of the position of the Gaussian excitation spot along the horizontal sample axis. The qualitative agreement with the experimental data shown in Fig. 8 clearly indicates that our interpretation of the effect is consistent with the SES measurements results.

6. Conclusion

Both VSL and SES measurements on silicon nanocrystal waveguides can be performed provided the careful experimental approach described here is applied. Monitoring both the pump diffraction effects and the signal collection efficiency, reliable data can be extracted from VSL technique. Positive gain and optical losses can be measured unambiguously in silicon nanocrystal waveguides, depending only on the pumping conditions. The observations of [12] have been reproduced on a sample of Si nanocrystals produced by a different growth technique and interpreted within a general propagation model.

Acknowledgements

This work has been supported by the INFM advanced research project RAMSES. We acknowledge Dr. Fabio Iacona for sample preparation in IMM CNR of Catania and Prof. Francesco Priolo and co-workers from Universita di Catania for helpful discussions. We thank Dr. Z. Gaburro for valuable technical helps.

References

- [1] K.L. Shaklee, R.E. Nahaori, L.F. Leheny, *J. Lumin.* 7 (1973) 284.
- [2] O. Svelto, S. Taccheo, C. Svelto, *Opt. Commun.* 149 (1998) 277.
- [3] L. Dal Negro, M. Cazzanelli, N. Daldosso, Z. Gaburro, L. Pavesi, F. Priolo, D. Pacifici, G. Franzò, F. Iacona, *Physica E* 16 (2003) 297.
- [4] L. Dal Negro, M. Cazzanelli, Z. Gaburro, P. Bettotti, L. Pavesi, F. Priolo, G. Franzò, D. Pacifici, F. Iacona, in: L. Pavesi, S. Gaponenko, L. Dal Negro (Eds.), *Towards the first silicon laser*, NATO Science Series, vol. 93, Kluwer Academic Publishers, Dordrecht, 2003; L. Dal Negro, M. Cazzanelli, L. Pavesi, S. Ossicini, D. Pacifici, G. Franzò, F. Priolo, F. Iacona, *Appl. Phys. Lett.* 82 (2003) 4636.
- [5] L. Khriachtchev, M. Rasanen, S. Novikov, J. Sinkkonen, *Appl. Phys. Lett.* 79 (2001) 1249.
- [6] P.W. Milonni, J.H. Eberly, *Lasers*, John Wiley & Sons, New York, 1988.
- [7] O. Svelto, D.C. Hanna, *Principles of Lasers*, Plenum Press, New York, 1998.
- [8] L. Pavesi, L. Dal Negro, C. Mazzoleni, G. Franzò, F. Priolo, *Nature* 408 (2000) 440.
- [9] L. Khriachtchev, S. Novikov, J. Lahtinen, *J. Appl. Phys.* 92 (2002) 5856.
- [10] M. Born, E. Wolf, *Principles of Optics*, seventh ed., Cambridge University Press, Cambridge, 1999.
- [11] F. Iacona, G. Franzò, C. Spinella, *J. Appl. Phys.* 87 (2000) 1295.
- [12] J. Valenta, I. Pelant, J. Linnros, *Appl. Phys. Lett.* 81 (2002) 1396.
- [13] P.C. Mogensén, P.M. Smowton, P. Blood, *Appl. Phys. Lett.* 71 (1997) 1975.
- [14] P.M. Smowton, E. Herrmann, Y. Ning, et al., *Appl. Phys. Lett.* 78 (2001) 2629.
- [15] L. Khriachtchev, M. Rasanen, in: L. Pavesi, S. Gaponenko, L. Dal Negro (Eds.), *Towards the first silicon laser*, NATO Science Series, vol. 93, Kluwer Academic Publishers, Dordrecht, 2003; L. Khriachtchev, M. Rasanen, S. Novikov, *Appl. Phys. Lett.* 83 (2003) 3018.